JOURNAL OF CHEMICAL INFORMATION AND MODELING

Article

pubs.acs.org/jcim

# Discovery of Novel Histamine H4 and Serotonin Transporter Ligands Using the Topological Feature Tree Descriptor

Róbert Kiss,[†,§] Márk Sándor,[†,§] Anikó Gere,[†] Éva Schmidt,[†] György T. Balogh,[†] Béla Kiss,[†] László Molnár,[†,∥] Christian Lemmen,[‡] and György M. Keserű*[,†]

[†]Gedeon Richter Plc, Gyömrői út 19-21, H-1103 Budapest, Hungary

[‡]BioSolveIT GmbH, An der Ziegelei 79, 53757 St. Augustin, Germany

Supporting Information

**ABSTRACT:** Ligand-based approaches are particularly important in the hit identification process of drug discovery when no structural information on the target is available. Pharmacophore descriptors that use a topological representation of the ligands are usually fast enough to screen large compound libraries effectively when seeking novel lead candidates. One example of this kind is the *Feature Tree* descriptor, a reduced graph representation implemented in the FTrees software. In this study, we tested the screening efficiency of FTrees by both retrospective and prospective screens using known histamine H4 antagonists and serotonin transporter (SERT) inhibitors as query molecules. Our results demonstrate that FTrees can effectively find actives. Particularly when combined with a subsequent 2D fingerprint-based diversity selection, FTrees was found to be extremely effective at discovering a diverse set of scaffolds. Prospective screening of our in-house compound deck provided several novel H4 and SERT ligands that could serve as suitable starting points for further optimization.

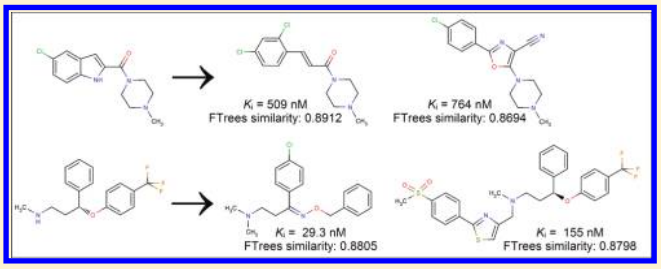


## 1. INTRODUCTION

As a complementary strategy to experimental approaches, virtual screening has become one of the key techniques in hit discovery. While the number of confirmed hits is typically lower than that of high-throughput screening (HTS), it can deliver valuable chemical starting points. The number of identified actives alone is not a useful performance metric for any screening technique. The chance of hits becoming promising leads depends on several other factors besides potency. One of these factors is their structural diversity from competitors' reference compounds. Particularly for ligand-based virtual screening, identified hits should differ from these reference query compounds by at least one crucial fragment. Such a "scaffold hop" allows for a differentiation in terms of chemistry, pharmacology, intellectual property, and more importantly, pharmacotherapy.

Ligand-based virtual screening approaches showing reasonable hit rates and providing structurally diverse chemotypes at the same time can therefore be particularly useful. Rather simplistic ligand-based models can be used effectively for compound library prefiltering, while more advanced techniques for extracting pharmacophoric properties of reference ligands may also yield favorable chemical starting points significantly faster than structure-based methods. Their application is therefore recommended even if structural information is available. In fact, some comparative studies suggest that they can be as or even more effective than structure-based virtual screening.[1] Furthermore, it was found that the potency of hits identified by ligand-based screens[2−4] is on average considerably higher than for structure-based screens.[5−10] In spite of this, structure-based virtual screening studies dominate in literature examples,[5] possibly because they are assumed to impose no structure-similarity bias and promise a maximum of diversity in the hit list.

Ligand-based approaches rely on the similarity principle and are based on various types of molecular descriptors ranging from simple physicochemical property counts to complex 3D molecular fields. Topological descriptors are positioned between these extremes. They combine the advantage of being quick to calculate, while preserving the connectivity information of the individual molecular fragments. Topological information can be stored in different ways, e.g., as bit string type molecular fingerprints. These allow for an application in large-scale database screening. Several topological descriptor-types are routinely used in pharmaceutical research for different purposes. Some of them were designed to identify close structural analogs [e.g., MACCS substructure keys (Accelrys, www.accelrys.com) and Unity 2D fingerprints (Tripos, www.tripos.com)], while others are suggested to be more suitable for scaffold hopping [e.g., FTrees (BioSolveIT, www.biosolveit.de) and CATS[11]].

FTrees is based on a noncyclic, topological descriptor (Feature Tree) that represents molecules by reduced graphs consisting of fragments (nodes) and their interconnecting bonds (edges).[12] Unlike fingerprints, the graph-based representation preserves the topology of the whole molecule. The nodes do not store detailed structural information on an atomic

**Received:** October 19, 2011
**Published:** December 14, 2011





dx.doi.org/10.1021/ci2004972 | J. Chem. Inf. Model. 2012, 52, 233−242

level, but they are labeled by the shape and chemical properties of the underlying fragment. The Feature Tree captures the pharmacophore information in a sufficiently fuzzy way to enable the identification of structurally dissimilar actives (i.e., scaffold hopping). Because of the topological nature of the descriptor, this approach avoids the uncertainties of 3D coordinate calculation and is significantly faster than 3D methods, permitting screens of large databases on a reasonable time scale.

Several publications suggest that the topological descriptor and screening technology of FTrees may yield high hit rates and are capable of scaffold hopping.[1,12,13] These literature examples prompted us to evaluate FTrees on two membrane-bound targets representing important target classes as GPCRs (histamine H4 receptor) and monoamine transporters [serotonin transporter (SERT)] by both retrospective and prospective screens. To the best of our knowledge, this is the first report of a prospective screen with FTrees.

## 2. MATERIALS AND METHODS

**FTrees.** The FTrees algorithm represents molecules as interconnected fragments.[12] These fragments are characterized by their shape (van der Waals volume and ring closure counts) as well as pharmacophore properties (numbers of H-bond donors/acceptors, delocalized systems, and hydrophobic sites). This way compounds are represented as noncyclic reduced graphs (Feature Trees), where the nodes correspond to the individual fragments joined by edges if the respective fragments are connected. Most importantly, rings are represented as single nodes, and a heuristic decomposes complex ring systems as interconnected nodes in such a way that the topology is optimally preserved while the Feature Tree remains cycle-free. Naturally, macrocycles cannot be well represented by Feature Trees. The properties of the nodes are coded as a numerical fingerprint, which provides an efficient way of assessing the "local" similarity of individual nodes as the Tanimoto coefficient of the respective fingerprints. The "global" Feature Tree similarity is determined on the basis of a mapping of the nodes of one Feature Tree onto the nodes of the other as the normalized sum of the local similarities of the mapped nodes. In our calculations, the so-called match−search algorithm[12] was used to calculate the mapping. Among all topology-preserving mappings, this algorithm determines the one with the highest global similarity, while providing two degrees of freedom: (a) neighboring nodes in one Feature Tree may be joined to map onto a single node of the other tree and (b) so-called NIL matches (node onto nothing) are permissible at the cost of a certain penalty, which is subtracted from the global similarity.

**Retrospective Screening.** For the retrospective tests, active compounds were mixed with decoys and enrichment tests were performed. The compound databases of four vendor companies, ChemBridge (www.chembridge.com), InterBioScreen (www.ibscreen.com), Asinex (www.asinex.com), and Maybridge (www.maybridge.com), were used. These contained 1.3 million compounds altogether. A total of 20,000 molecules of these were randomly selected as "decoys". LigPrep 2.2 (Schrödinger, www.schrodinger.com) was used to eliminate salts and generate the most probable protomer and tautomeric form at pH 7. InChI identifiers of these ligands were generated by the InChI 1.02 software [IUPAC's (International Union of Pure and Applied Chemistry) International Chemical Identifier, www.inchi-trust.org] to remove duplicates. The remaining 19,791 ligands were used as decoys in the enrichment tests.

As "actives", 58 histamine H4 receptor (H4) antagonists and 274 serotonin transporter (SERT) inhibitors were collected from Thomson Reuters Integrity database (Thomson Reuters, integrity.thomson-pharma.com). These ligands were prepared for virtual screening by LigPrep in a similar way as the decoys. Using default settings, Feature Tree descriptors were calculated using FTrees version 2.0, and 2D structural fingerprints were calculated by Unity in Sybyl 8.0 (Tripos, www.tripos.com). Similarity matrices for both descriptors were calculated using the respective methods, and the virtual screening performance was assessed by selecting different "active sets" as follows: (i) all actives were selected, (ii) 10 actives were randomly selected, (iii) the 10 most diverse actives based on the FTrees similarities were selected, and (iv) the 10 most diverse actives based on the Unity similarities were selected. In all enrichment tests, one active at a time was selected as the query compound with the aim of finding the remaining actives from the respective active set. This test was repeated for each active in the active set. Average enrichment factors (EFs) for each active set definitions were calculated at the top 10%, 5%, 2%, 1%, 0.50%, and 0.10% of the screened database. Here, the database is sorted by the respective similarity value, and only the top X% fraction considered. EF is then defined as the percentage of actives retrieved divided by the percentage fraction of the database considered. This value reflects at which rate more actives are retrieved as compared to a random selection (X% actives at X% of the database → EF = 1). These EFs correspond to an application scenario when only one query compound is available (single active evaluation).

As an alternative scenario, when multiple query compounds are available, we calculated the similarity matrix on the basis of the maximum similarity. This is defined as the highest similarity value to any one of the query compounds. All actives from the respective active set were used as queries (multiple actives evaluation). However, the self-similarity of the active used as the query was excluded. A similar evaluation strategy was applied by Evers et al.,[1] where the higher similarity from two independent query models (winner score) was used for ranking.

**Prospective Screening.** In order to complement these retrospective analyses, we evaluated the screening deck of Gedeon Richter comprising 148,780 compounds using FTrees with two H4 and two SERT molecules as queries. All molecules were prepared as described above for the retrospective tests. After calculating the FTrees similarity to each query molecule, at most only 1000 compounds per query, with an FTrees similarity above 0.85, were retained as preliminary hits. For these, Unity 2D fingerprints and corresponding Tanimoto coefficients were used to select a structurally diverse subset (at most 50 compounds per query molecule) for in vitro testing.

**Histamine H4 Radioligand Binding Assay.** SK-N-MC cells transfected with human H4 receptor were collected with PBS and centrifuged at 3000 *g* for 10 min at 4 °C. Pellets were collected and homogenized in 50 mM Tris pH 7.5 containing 5 mM EDTA. After centrifugation at 40,000 *g* (25 min at 4 °C), pellets were rehomogenized in 50 mM Tris pH 7.5 containing 5 mM EDTA, aliquoted, and stored at −70 °C until use. For the H4 competition binding studies, cell membranes were incubated in plastic tubes with 10 nM [$^3$H]histamine with or without test compounds for 60 min at 25 °C. Nonspecific binding was defined using 100 $\mu$M unlabeled histamine. After incubation, the membranes were filtered through GF/C filters pretreated with 0.5% polyethylenimine using an M48 Brandel cell harvester. Filters were placed into a scintillation cocktail

(OPTIPHASE "HISAFE" 3, PerkinElmer) and quantified by a Tri-Carb 2900TR liquid scintillation spectrometer (PerkinElmer). Data were analyzed using GraphPad Prism (Graph-Pad Software, San Diego, CA, www.graphpad.com). Initial screening involved the measurement of [$^3$H]histamine displacement at 2 $\mu$M. $K_i$ values for compounds with [$^3$H]histamine displacement over 20% and purity over 90% were calculated according to Cheng and Prusoff.[14]

**Serotonin Transporter Binding Assay.** Male Sprague–Dawley rats weighing 180–220 g were used for the measurement of SERT binding. Rats were purchased from WOBE Ltd. (Harlan, Europe). Animals arrived in the laboratory at least two days before the experiment. All the procedures carried out on animals had been approved by the local ethical committee and conformed to the rules and principles of the 86/609/EEC Directive. SERT binding was determined according to the method described by D'Amato et al.[15] and Owens et al.[16] with some modification. Rats were decapitated, brains were rapidly removed and chilled in ice-cold saline then cerebellum, and pons-medulla were removed and immediately frozen in dry ice. Forebrain (whole brain minus cerebellum and pons-medulla) was homogenized in 25 vol ice-cold buffer containing 50 mM Tris-HCl buffer (pH 7.4, 25 °C; 120 mM NaCl; 5 mM KCl), and the homogenate was centrifuged at 45,000 *g* for 10 min at 4 °C. The pellet was suspended in the same buffer and was centrifuged at 45,000 *g* for 10 min at 4 °C. The membrane was washed once more in the same buffer, and the pellet was resuspended in 25 vol ice-cold buffer at a final concentration of 2.7 mg protein/mL. Membrane preparation was stored at −70 °C until use in 4.5 mL of aliquot.

For binding assay, aliquot of membrane (4.5 mL) was thawed, diluted with 16.5 mL of buffer (50 mM Tris-HCl buffer, pH 7.4, 25 °C; 120 mM NaCl; 5 mM KCl), and then homogenized using Dounce homogenizer. A total of 0.2 mL membrane suspension (containing 0.12 mg protein) was incubated with 1 nM [$^3$H]citalopram (70 Ci/mmol, PerkinElmer, NET-1039) in the presence or absence of different concentrations of compounds for 1 h at room temperature. The final incubation volume was 0.25 mL. Nonspecific binding, assessed in the presence of paroxetine (0.5 $\mu$M), was 2–4% of the total binding. The assay was stopped by filtration on a Unifilter-96 GF/B filter (PerkinElmer Boston, MA, www.perkin-elmer.com) presoaked for 2–3 h in 0.5% polyethylene-imine solution before use. The filters were washed 3 times with 5 mL of ice-cold buffer (50 mM Tris-HCl buffer, pH 7.4, 25 °C; 120 mM NaCl; 5 mM KCl), and radioactivity of the filters was counted by liquid scintillation spectrometry in 40 $\mu$L of MicroScint-20 (PerkinElmer) scintillation cocktail using a TopCount NXT microplate scintillation and luminescence counter (Packard). Initial screening of [$^3$H]citalopram displacement was measured at 2 $\mu$M. $K_i$ values for compounds with [$^3$H]citalopram displacement over 20% and purity over 90% were calculated using the Cheng-Prusoff equation.[14]

**Purity and Identity Assessment of in Vitro Hits.** LC-MS experiments were carried out on an Agilent 1200 liquid chromatography system coupled with an 6120 MSD (Agilent, www.agilent.com), equipped with a vacuum degasser, binary pump, autosampler, column temperature controller, and diode array detector. Analysis was at 40 °C on a Kinetex $C_{18}$ column (5 cm × 2.1 mm, 2.6 $\mu$m) (Phenomenex, www.phenomenex.com) with a mobile phase flow rate of 0.9 mL/min. Composition of eluent A was 0.1% (v/v) trifluoroacetic acid in water (pH 1.9), and eluent B was the mixture of acetonitrile and water in 95:5 (v/v) with 0.1% (v/v) trifluoroacetic acid. A fast linear gradient of 0–100% B was applied at a range of 0–4 min, and then 100% B was held for 3 min. This was followed by a 2 min equilibration period prior to the next injection. The injection volume was set at 1 $\mu$L, and the sample concentration was uniformly 1.0 mg/mL (solved in DMSO). The UV–vis spectra were recorded between 200 and 400 nm, and the chromatographic profile was registered at 240 nm. The MSD operating parameters were as follows: positive ionization mode, scan spectra from $m/z$ 100 to 800, drying gas temperature 350 °C, nitrogen flow rate 12 L/min, nebulizer pressure 60 psi, quadrupole temperature 100 °C, capillary voltage 3000 V, and fragmentor voltage 50 V.

NMR measurements were performed on a Varian 500 MHz NMR spectrometer equipped with a $^1$H {$^{13}$C/$^{15}$N} 5 mm PFG Triple Resonance $^{13}$C Enhanced Cold Probe and on a Varian 800 MHz NMR spectrometer equipped with a $^1$H{$^{13}$C/$^{15}$N} Triple Resonance $^{13}$C Enhanced Salt Tolerant Cold Probe operating at 500 and 800 MHz for $^1$H nucleus, respectively.

In the case of compounds available in solid form, $CDCl_3$ (Merck, Darmstadt, Germany) was used as solvent, and standard 5 mm NMR tubes were used. In the case of samples available only in 1 mg/mL DMSO-h6 solution, 100 $\mu$L of solution was diluted with 150 $\mu$L of DMSO-d6 (Merck, Darmstadt, Germany), and 5 mm Shigemi tubes were utilized. Chemical shifts are reported in ppm using either TMS or DMSO-h6 (2.55 ppm) as internal references. All NMR experiments were performed at 298 K using standard pulse sequences available in the VNMRJ program suite. For compounds available in solid form, $^1$H–$^1$H, direct $^1$H–$^{13}$C, scalar, and dipolar spin–spin connectivities were established from $^1$D $^1$H, NOESY, zTOCSY, and 2D gHSQCAD NMR experiments. In the case of samples available in DMSO-h6 solutions, only $^1$H NMR data could be collected with the suppression of the DMSO-h6 and residual water signals using the standard WET solvent suppression sequence. In some cases not all the $^1$H NMR resonances could be detected due to signal overlaps with the solvent resonances.

## 3. RESULTS AND DISCUSSION

**Retrospective Screening.** We started the evaluation of FTrees by retrospective screens and compared its performance with that of Unity 2D fingerprints (Unity FP). These two methods are quite orthogonal as the former claims to be suitable for scaffold hopping, while the latter was designed to identify close structural analogs.[17−19]

**Enrichment Tests.** The "active set" of the enrichment studies was selected in different ways: (i) all actives were selected, (ii) 10 actives were randomly selected, (iii) the 10 most diverse actives based on the FTrees similarities were selected, and (iv) the 10 most diverse actives based on the Unity similarities were selected.

Including all H4 antagonists and SERT inhibitors that were available in the Prous Integrity database (58 H4 and 274 SERT compounds), we obtained quite high enrichment factors (EFs) for both methods (Table 1 and Figure 1).

The high, in some cases optimal, EFs suggest that both methods, FTrees and Unity FP, are capable of retrieving known actives from large data sets for both targets. Not surprisingly, the multiple actives evaluation yielded significantly higher enrichments than the single active evaluation scenario. This can be explained by the heightened probability that the active set will contain at least one highly similar query to any one of the actives.


dx.doi.org/10.1021/ci2004972 | J. Chem. Inf. Model. 2012, 52, 233–242

Table 1. Enrichment Factors (EF) Calculated for the Top 10%, 5%, 2%, 1%, 0.50%, and 0.10% of the Screened Databases[a]

| target | screening method | active set | single (S) or multiple (M) actives eval. | EF at top 10% | EF at top 5% | EF at top 2% | EF at top 1% | EF at top 0.5% | EF at top 0.1% |
|---|---|---|---|---|---|---|---|---|---|
| H4 | FTrees | All actives | S | 5.8 (10.0) | 10.3 (20.0) | 22.4 (50.0) | 37.8 (100.2) | 60.6 (200.5) | 163.0 (348.2) |
| | | | M | 10.0 (10.0) | 19.3 (20.0) | 48.3 (50.0) | 96.8 (100.2) | 186.7 (200.5) | 325.1 (342.2) |
| | | 10 random | S | 6.2 (10.0) | 10.7 (20.0) | 25.0 (50.0) | 43.3 (100.0) | 84.4 (200.0) | 253.0 (990.0) |
| | | | M | 10.0 (10.0) | 20.0 (20.0) | 50.0 (50.0) | 100.0 (100.0) | 140.0 (200.0) | 495.0 (990.1) |
| | | 10 diverse (FTrees) | S | 4.1 (10.0) | 6.7 (20.0) | 12.2 (50.0) | 14.4 (100.0) | 22.2 (200.0) | 0.0 (990.0) |
| | | | M | 3.0 (10.0) | 6.0 (20.0) | 0.0 (50.0) | 0.0 (100.0) | 0.0 (200.0) | 0.0 (990.1) |
| | | 10 diverse (Unity FP) | S | 5.0 (10.0) | 8.4 (20.0) | 17.2 (50.0) | 24.4 (100.0) | 42.2 (200.0) | 99.0 (990.0) |
| | | | M | 10.0 (10.0) | 18.0 (20.0) | 35.0 (50.0) | 60.0 (100.0) | 80.0 (200.0) | 396.0 (990.1) |
| | Unity FP | All actives | S | 5.1 (10.0) | 8.5 (20.0) | 18.2 (50.0) | 32.3 (100.2) | 57.6 (200.5) | 182.8 (348.2) |
| | | | M | 10.0 (10.0) | 20.0 (20.0) | 50.0 (50.0) | 98.5 (100.2) | 186.7 (200.5) | 325.1 (342.2) |
| | | 10 random | S | 4.2 (10.0) | 5.8 (20.0) | 11.1 (50.0) | 16.7 (100.0) | 31.1 (200.0) | 121.0 (990.0) |
| | | | M | 9.0 (10.0) | 18.0 (20.0) | 45.0 (50.0) | 70.0 (100.0) | 140.0 (200.0) | 495.0 (990.1) |
| | | 10 diverse (FTrees) | S | 5.7 (10.0) | 9.3 (20.0) | 16.1 (50.0) | 26.7 (100.0) | 42.2 (200.0) | 165.0 (990.0) |
| | | | M | 9.0 (10.0) | 14.0 (20.0) | 25.0 (50.0) | 50.0 (100.0) | 100.0 (200.0) | 396.0 (990.1) |
| | | 10 diverse (Unity FP) | S | 3.7 (10.0) | 6.7 (20.0) | 12.2 (50.0) | 12.2 (100.0) | 17.8 (200.0) | 66.0 (990.0) |
| | | | M | 8.0 (10.0) | 10.0 (20.0) | 25.0 (50.0) | 50.0 (100.0) | 80.0 (200.0) | 0.0 (990.1) |
| SERT | FTrees | All actives | S | 4.0 (10.0) | 5.7 (20.0) | 9.2 (50.0) | 13.0 (73.5) | 18.0 (73.5) | 37.6 (73.5) |
| | | | M | 9.6 (10.0) | 19.0 (20.0) | 44.2 (50.0) | 72.5 (73.2) | 72.5 (73.2) | 69.6 (73.2) |
| | | 10 random | S | 2.7 (10.0) | 3.6 (20.0) | 6.1 (50.0) | 11.1 (100.0) | 20.0 (200.0) | 55.0 (990.0) |
| | | | M | 7.0 (10.0) | 12.0 (20.0) | 15.0 (50.0) | 20.0 (100.0) | 40.0 (200.0) | 198.0 (990.1) |
| | | 10 diverse (FTrees) | S | 1.7 (10.0) | 0.9 (20.0) | 0.0 (50.0) | 0.0 (100.0) | 0.0 (200.0) | 0.0 (990.0) |
| | | | M | 0.0 (10.0) | 0.0 (20.0) | 0.0 (50.0) | 0.0 (100.0) | 0.0 (200.0) | 0.0 (990.1) |
| | | 10 diverse (Unity FP) | S | 1.3 (10.0) | 0.9 (20.0) | 0.6 (50.0) | 1.1 (100.0) | 2.2 (200.0) | 0.0 (990.0) |
| | | | M | 0.0 (10.0) | 0.0 (20.0) | 0.0 (50.0) | 0.0 (100.0) | 0.0 (200.0) | 0.0 (990.1) |
| | Unity FP | All actives | S | 4.7 (10.0) | 6.8 (20.0) | 10.6 (50.0) | 14.6 (73.5) | 20.6 (73.5) | 40.8 (73.5) |
| | | | M | 9.8 (10.0) | 19.2 (20.0) | 46.0 (50.0) | 71.8 (73.2) | 72.5 (73.2) | 69.6 (73.2) |
| | | 10 random | S | 4.2 (10.0) | 4.9 (20.0) | 7.2 (50.0) | 8.9 (100.0) | 13.3 (200.0) | 33.0 (990.0) |
| | | | M | 7.0 (10.0) | 8.0 (20.0) | 10.0 (50.0) | 20.0 (100.0) | 40.0 (200.0) | 198.0 (990.1) |
| | | 10 diverse (FTrees) | S | 4.2 (10.0) | 5.6 (20.0) | 8.3 (50.0) | 8.9 (100.0) | 6.7 (200.0) | 11.0 (990.0) |
| | | | M | 4.0 (10.0) | 8.0 (20.0) | 0.0 (50.0) | 0.0 (100.0) | 0.0 (200.0) | 0.0 (990.1) |
| | | 10 diverse (Unity FP) | S | 1.7 (10.0) | 0.9 (20.0) | 1.1 (50.0) | 2.2 (100.0) | 0.0 (200.0) | 0.0 (990.0) |
| | | | M | 0.0 (10.0) | 0.0 (20.0) | 0.0 (50.0) | 0.0 (100.0) | 0.0 (200.0) | 0.0 (990.1) |

[a]Maximum achievable EFs are provided for reference in brackets.

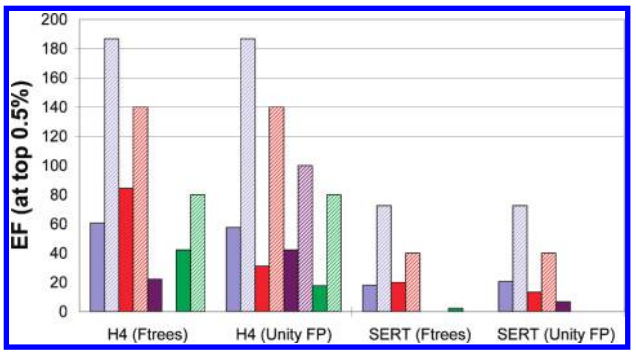


**Figure 1.** Enrichment factors (EF) calculated at top 0.5% of the database for active sets: "All actives" (blue), "10 random" (red), "10 dissimilar (FTrees)" (purple), and "10 dissimilar (Unity FP)" (light green). EFs for the single active evaluation are indicated with full colors, while the bars with striped colors show the EFs for the multiple actives evaluation.

As further tests, we randomly selected a small portion (10 compounds) of the available actives to decrease the maximum similarity of the active sets (Tables 1 and 2).

While the average similarity of the 10 randomly selected actives was not significantly different from that among all actives, the maximum similarity in the set was significantly lower due to the reduced probability of randomly selecting two close analogs (Table 2). Interestingly, we see a distinct decrease in enrichments with Unity FP (both in single active and multiple actives evaluations), while no such trend can be identified with FTrees.

We also conducted screens where the active set comprised diverse actives selected by the respective other descriptor. We first tested if FTrees was able to identify Unity FP diverse actives and vice versa. Interestingly, we found similarly high EFs in the H4 screens for both descriptors, while neither of them showed reasonable performance with SERT ligands in this scenario (Table 1 and Figure 1).

Finally, we analyzed the performance of FTrees and Unity FP with active sets generated by the same method used for the screening. An ideally discriminating method should find all actives more similar than any inactive, no matter how diverse the active set. However, not surprisingly, in reality this setup significantly lowered all EFs. Interestingly, quite high enrichments were still found with Unity FP in the case of the H4 screens (Table 1 and Figure 1).

The same number of actives and decoys used in three of the four scenarios [10 random, 10 diverse (FTrees), and 10 diverse (Unity FP)] allows for a direct comparison of EFs on the two targets. This shows that EFs were significantly higher for the


dx.doi.org/10.1021/ci2004972 | J. Chem. Inf. Model. 2012, 52, 233−242

**Table 2. Calculated Average, Maximum, and Minimum Similarity Values (FTrees and Unity FP) among the Actives for the respective H4 and SERT Active Sets**

| target | screening method | active set | average similarity ± S.D. | maximum similarity | minimum similarity |
|---|---|---|---|---|---|
| H4 | FTrees | All actives | 0.77 ± 0.10 | 1.00 | 0.49 |
| | | 10 random | 0.81 ± 0.09 | 0.95 | 0.63 |
| | | 10 diverse (FTrees) | 0.71 ± 0.07 | 0.84 | 0.54 |
| | | 10 diverse (Unity FP) | 0.71 ± 0.10 | 0.94 | 0.49 |
| | Unity FP | All actives | 0.41 ± 0.17 | 1.00 | 0.16 |
| | | 10 random | 0.37 ± 0.14 | 0.84 | 0.24 |
| | | 10 diverse (FTrees) | 0.37 ± 0.13 | 0.80 | 0.21 |
| | | 10 diverse (Unity FP) | 0.32 ± 0.08 | 0.55 | 0.16 |
| SERT | FTrees | All actives | 0.73 ± 0.08 | 1.00 | 0.45 |
| | | 10 random | 0.73 ± 0.07 | 0.99 | 0.63 |
| | | 10 diverse (FTrees) | 0.67 ± 0.06 | 0.79 | 0.50 |
| | | 10 diverse (Unity FP) | 0.68 ± 0.06 | 0.80 | 0.51 |
| | Unity FP | All actives | 0.37 ± 0.10 | 1.00 | 0.15 |
| | | 10 random | 0.35 ± 0.08 | 0.65 | 0.22 |
| | | 10 diverse (FTrees) | 0.35 ± 0.07 | 0.50 | 0.25 |
| | | 10 diverse (Unity FP) | 0.27 ± 0.05 | 0.35 | 0.17 |

H4 screens. This difference in performance suggests that both the FTrees and Unity FP methodology work better with currently available H4 ligands. Potentially, these compounds exhibit a higher degree of pharmacophore and structural similarity than the SERT ligands. This is also supported by the higher average and maximum similarity values in the H4 active sets compared to those of the SERT actives (Table 2). The smaller total number of available H4 antagonists (58 vs 274 SERT inhibitors) could also represent a lower number of active chemotypes. A random selection of 10 actives therefore may find compounds from the same class with higher probability.

In summary, both FTrees and Unity FP show significant enrichments over random on both targets, with higher EFs achieved on H4. We obtained quite high enrichment factors (EFs) for active sets (i) and (ii), while more diverse active sets yield significant enrichment in H4 screens only. The use of multiple actives yields generally better results than the use of a single active query compound. However, both methods also show reasonable performance when only a single active query is used. This suggests that they can be effective in projects at very early stages where only limited ligand information is available.

**Scaffold Hopping.** High enrichment factors achieved in the retrospective studies suggest that both FTrees and Unity FP are capable of identifying active compounds in large databases. However, it is also important to know whether these identified hits are suitable as chemical starting points for further optimization. One crucial factor in this regard is the structural similarity/dissimilarity between the query compound and the identified hit, i.e., whether or not such a pair of molecules comprises a scaffold hop. We therefore visually inspected those cases where FTrees and Unity FP yielded highest enrichments with single query compounds and randomly selected active sets and analyzed whether new scaffolds or only structural analogs were identified. For this purpose, all molecules were drawn by Marvin 5.4.1.0 (ChemAxon, www.chemaxon.com).

In the case of the H4 screens (Figure 2 and Figure S1 of the Supporting Information), the FTrees search with a benzimidazole query (compound **1**) yielded the highest EFs (440 at top 0.1% and 133 at top 0.5%). Two hits containing indole (**2**) and thienopyrrole (**5**) functionalities were found to be structurally similar to the query compound. Accordingly, they have higher than average (0.37 for the H4 10 random active set) Unity FP similarities (0.49 for compound **2** and 0.38 for compound **5**) (Figure 1 and Table 2). The remaining four hits represented three completely different scaffolds: quinoxaline (compound **3**), amino-pyrimidine (**4** and **6**), and benzofuropyrimidine (**7**). These latter compounds exhibit also much lower Unity FP similarities (0.28, 0.35, 0.34, and 0.31 for compounds **3**, **4**, **6**, and **7**, respectively), which confirms their structural distinction from the query compound. Altogether, two-thirds of the hits retrieved by FTrees show clear scaffold hops. Interestingly, the hop from the indole (**2**) to the quinoxaline (**3**) scaffold was reported by Smits et al. by using a flexible alignment model.[20] Further interpreting this model led to another scaffold hop, i.e., the identification of quinazolines.[21] In another interesting study, a vendor library was screened against compound **2** by using CATS pharmacophore descriptors and some moderately active hits were identified. Fragments of these hits and H4 reference ligands were successfully combined by a scaffold hopping approach resulting in potent 2,4-diaminopyrimidines.[22]

Unity FP showed the highest EFs with an amino-pyrimidine derivative query (compound **8**). Here, two out of the nine actives could be identified at the top 0.1% of the database (EF = 220) and one further active at 0.5% (EF = 67). The highest ranked two actives (**4** and **6**) are close analogs to the query molecule sharing the same 2-amino-pyrimidine scaffold. However, the third hit (compound **7**), which has a benzofuropyrimidine ring system, can be considered a moderate scaffold hop. Interestingly Cramp and co-workers also reported the successful identification of the benzofuropyrimidine scaffold by pharmacophore screening[23] against compound **2** (JNJ-7777120).[24]

SERT screens (Figure 3 and Figure S2 of the Supporting Information) resulted in significantly lower EFs compared to those achieved with H4. The highest EFs for FTrees (220 at top 0.1% and 44 at top 0.5%) and Unity FP (110 at top 0.1% and 44 at top 0.5%) were found with very similar 8-azabicyclo[3.2.1]octane derivatives (compounds **9** and **10**). The highest ranked compound for both methods was the query used by the respective other method (i.e., compound **10** for FTrees and compound **9** for Unity FP). Both FTrees and Unity FP were able to scaffold hop by identifying compounds **11** and **12**, which are structurally considerably different from either query.

In summary, FTrees could identify three (H4) and one (SERT) novel scaffolds, while Unity FP only yielded one moderately (H4) and one completely (SERT) novel scaffolds at the top 0.5% of the analyzed data sets. Furthermore, two out of the three (H4) and one (SERT) novel scaffolds found by FTrees were ranked in the top 0.1% of the database, while no new scaffold could be found by Unity FP at the top 0.1% level. It is also important to mention that the ratio of the actives in these test sets was relatively low (0.045%) and, therefore, recovering any actives at the top 0.1 or 0.5% of these sets means a very effective screening performance as reflected by the comparatively high enrichment factors.


dx.doi.org/10.1021/ci2004972 | J. Chem. Inf. Model. 2012, 52, 233−242

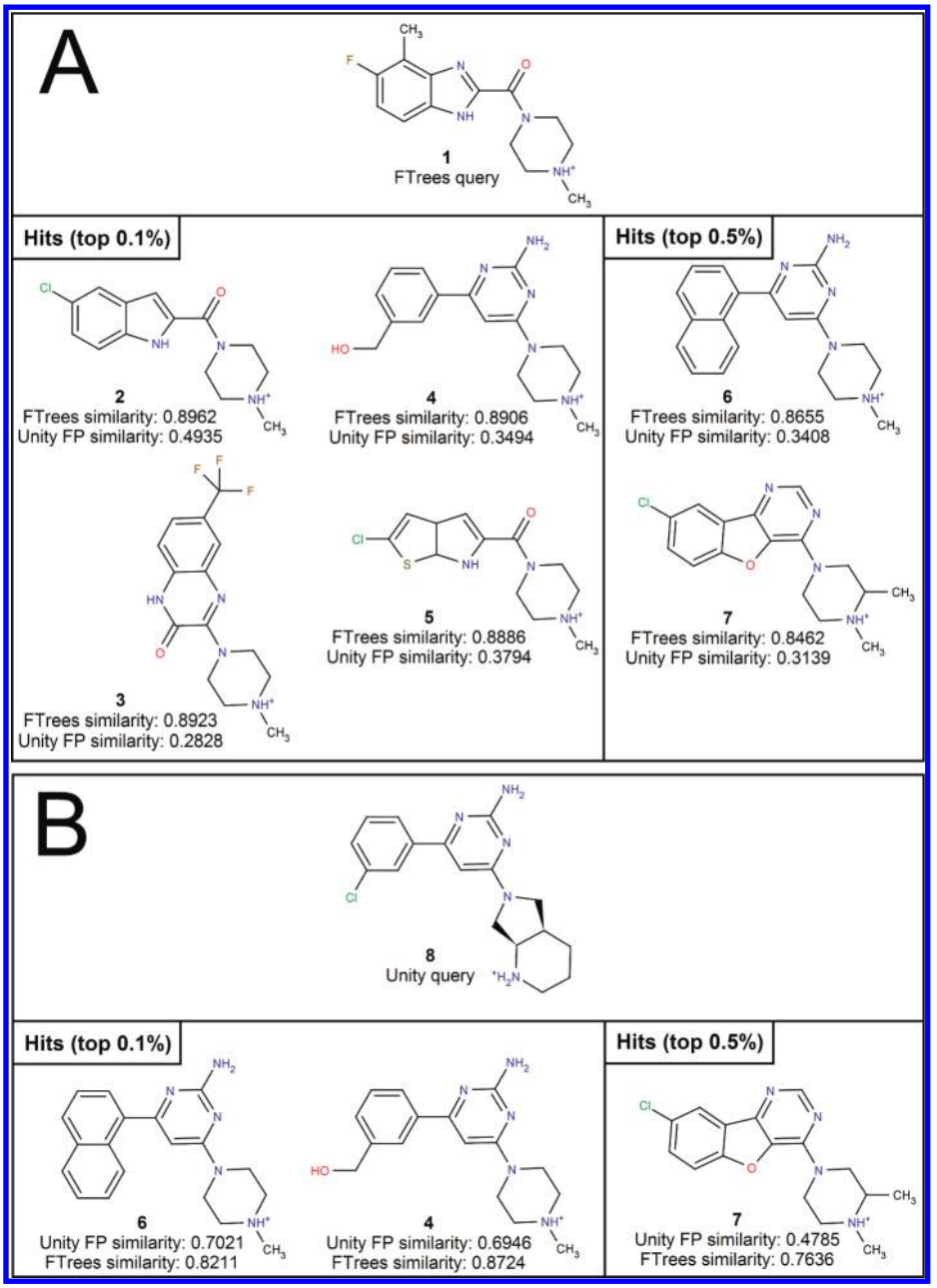


**Figure 2.** All active hits retrieved with H4 query compounds by FTrees (A) and Unity FP (B) in the top 0.1% and top 0.5% fractions of the data set.

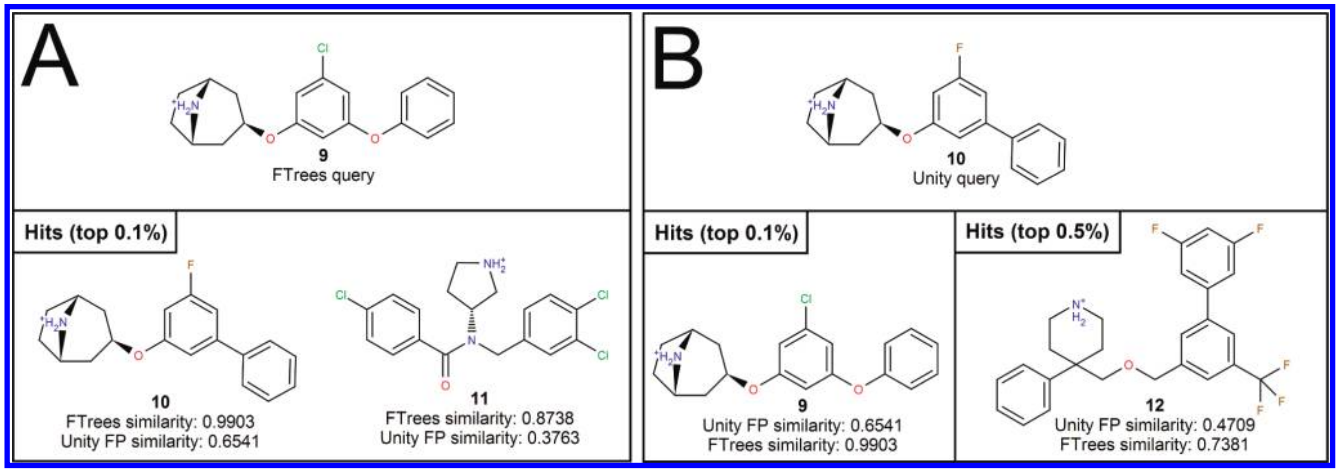


**Figure 3.** All active hits retrieved with SERT query compounds by FTrees (A) and Unity FP (B) in the top 0.1% and top 0.5% fractions of the data set.


dx.doi.org/10.1021/ci2004972 | J. Chem. Inf. Model. 2012, 52, 233−242

**Prospective Screening.** We concluded from the retrospective studies that both FTrees and Unity FP can yield impressive hit rates. Higher enrichments were achieved by using multiple actives as queries. However, the performance was also good with single query molecules. Because we were primarily interested in the application of these methods in the very early stages of drug discovery projects where at best only a few active compounds are typically available, we selected two H4 and two SERT query molecules for the prospective screens. As we further found that FTrees is more suitable for scaffold hopping while Unity FP usually identifies close structural analogs, we combined the two methods in a workflow to maximize likelihood of discovering novel scaffolds. First, we screened our corporate database against the two pairs of query molecules by FTrees. Subsequently, we selected a structurally diverse subset of the FTrees hits by using the Unity FP.

*H4.* We selected the first reported H4 antagonist (compound **2**)[24] and one representative from the amino-pyrimidine family (compound **15**)[25,26] as query compounds (Figure 4).

After screening our in-house compound set by FTrees, we selected compounds with similarity values above 0.85 (718 for query compound **2** and 152 for query compound **15**). 50 maximally diverse compounds from either subset were selected for in vitro testing based on Unity FP. Of these, 35 for query compound **2** and 33 for query compound **15** were available for immediate in vitro screening. The pharmacological screens identified three hits (two for query compound **2** and one for query compound **15**) with significant H4 activity (Figure 4). This represents a hit rate of 4.4% (5.7% for query compound **2** and 3.0% for query compound **15**), which is comparable with the hit rate of our previously published structure-based virtual screening study on the homology model of H4 receptor (6.3%).[6] It is important to mention that both H4 hits discovered by query compound **2** have $K_i$ values in the submicromolar range.

The identified hits as well as the query compounds all contain a piperazine group, which is believed to serve as a positively charged counterpart of the negatively charged groups of either Asp94 (3.32) (Ballesteros-Weinstein numbering)[27] or Glu182 (5.46) at the H4 receptor binding site.[28,29] On the other hand, the adjacent parts of all three hits represent considerable structural differences compared to the query molecules, which enables their further exploration.

*SERT.* For the SERT prospective screens, we selected a well-known SERT inhibitor (fluoxetine: compound **17**) and a recently published molecule containing an interesting benzenesulfonamide scaffold (compound **20**).[30] After the screening with FTrees, the highest ranked 1000 compounds from either query (all had FTrees similarities above 0.85) were subjected to diversity selection by Unity FP. The finally selected 50 compounds for either query shared two identical hits; therefore, 98 compounds were suggested for in vitro testing. Of these, 88 were available (46 for query compound **17** and 44 for compound **20**). Four in vitro hits (two for either query) showed significant SERT inhibition (Figure 5). This corresponds to a hit rate of 4.5% (4.3% for query compound **17** and 4.5% for query compound **20**).

Similar to the H4 screens, we found several compounds with submicromolar affinities (compounds **18**, **19**, and **21**). Manepalli et al. recently reported the identification of two moderately active SERT inhibitors ($K_i$ = 10−40 $\mu$M) by structure-based pharmacophore screening.[31] The remarkably high affinities in our study show the potential of ligand-based approaches to identify more potent hits than structure-based approaches as suggested by a recent comprehensive survey of prospective virtual screens.[5] While compound **19** is an analog of the query, compounds **18**, **21**, and **22** represent scaffolds significantly different from the queries, which suggests them as suitable candidates for further investigations.

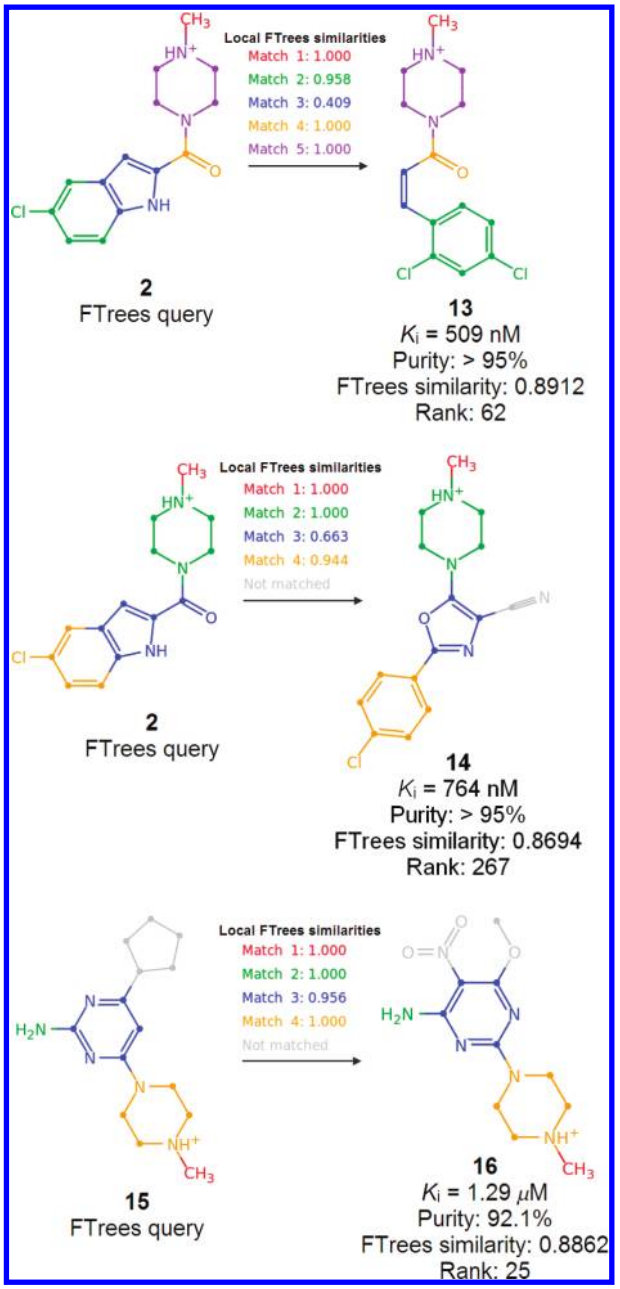


**Figure 4.** Novel H4 ligands discovered by FTrees. Matched Feature Tree nodes are indicated by the same coloring.

Interestingly, the identified SERT inhibitors as well as the query molecules share some characteristic SERT pharmacophoric features, such as two aromatic groups and a cationic nitrogen.[32−35] The topological distance between the aromatic groups and the positively charged nitrogen varies between 4 and 7 bonds, which is comparable to the 4-bond distance in the endogenous ligand, serotonin. The most potent hits contain halogens (Cl, $CF_3$, Br) similar to the query compounds ($CF_3$). This is in agreement with the findings of Gundertofte and coworkers,[32] who identified fluor-substitutions on the aromatic rings as favorable attributes of the SERT affinity.


dx.doi.org/10.1021/ci2004972 | J. Chem. Inf. Model. 2012, 52, 233−242

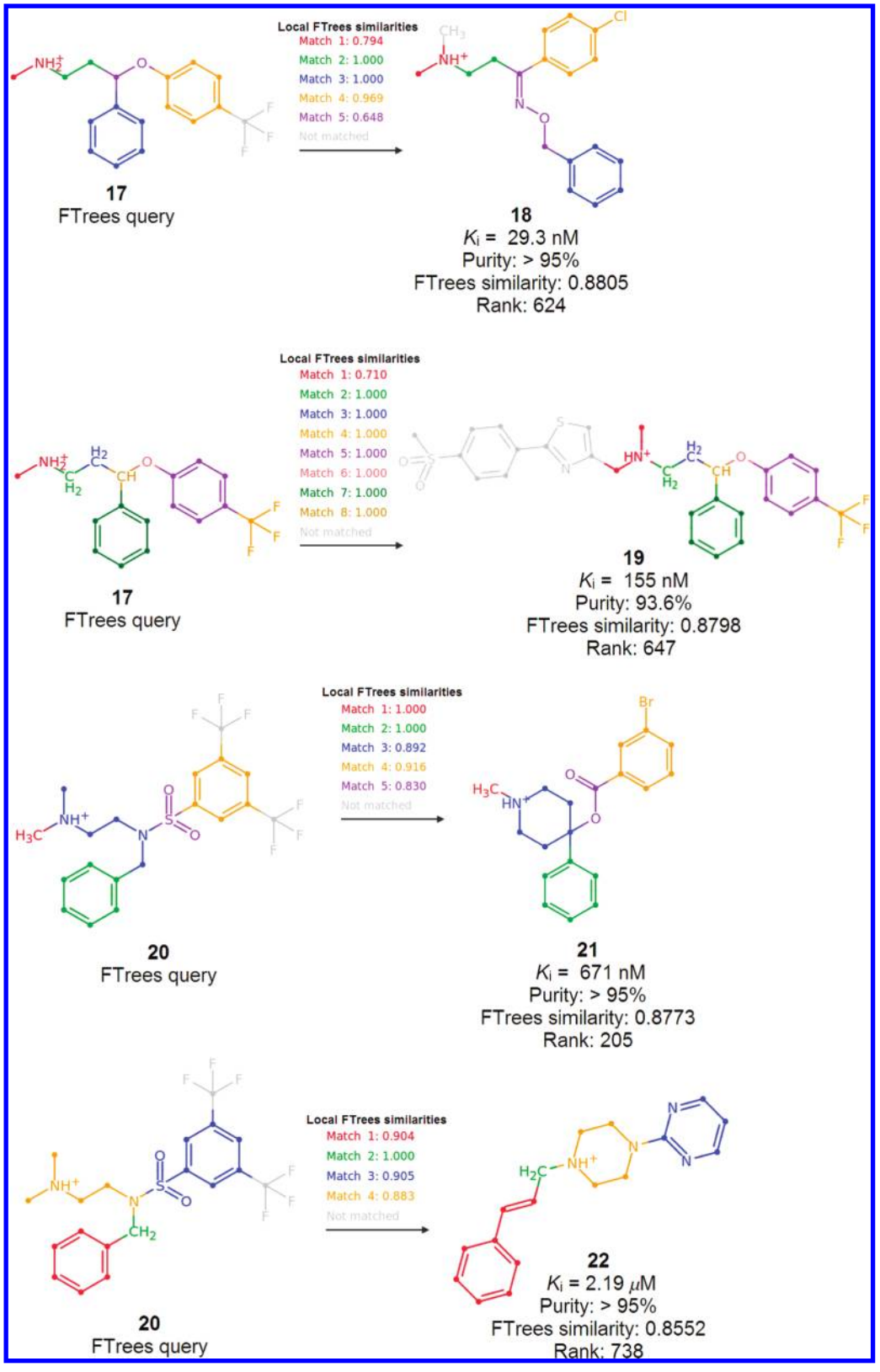


**Figure 5.** Novel SERT ligands discovered by FTrees. Matching Feature Tree nodes are indicated by the same coloring.

## 4. CONCLUSIONS

In this study, we evaluated the screening performance of FTrees and Unity 2D fingerprints in terms of enrichment factors and scaffold hopping capability by both retrospective and prospective studies. We found that the topological pharmacophore descriptor of FTrees more frequently identifies actives that are structurally different from the query compounds. Combining the strength of both methods, we performed the virtual screening using FTrees followed by a diversity selection based on the Unity FP. This workflow


dx.doi.org/10.1021/ci2004972 | J. Chem. Inf. Model. 2012, 52, 233−242

yielded reasonably high hit rates and revealed novel scaffolds that are suitable for further optimization on both of the targets under consideration. Our results suggest that FTrees can be a valuable tool in the hit identification process, especially but not necessarily limited to cases where 3D structural information about the target is not available. Our study was based on two membrane-bound targets representing important target classes as GPCRs (histamine H4 receptor) and monoamine transporters (serotonin transporter). To the best of our knowledge, this is the first published prospective screening study conducted on SERT as well as the first report of a prospective screen involving FTrees. The combined method shown here is able to identify novel chemical starting points in early stage drug discovery projects when usually at best only a limited number of active molecules is available.

## ■ ASSOCIATED CONTENT

### Supporting Information

Additional material for the retrospective virtual screening. This material is available free of charge via the Internet at http://pubs.acs.org.

## ■ AUTHOR INFORMATION


### Corresponding Author

*E-mail: gy.keseru@richter.hu. Fax: +36-1-4326002. Phone: +36-1-4314605.

### Present Addresses

[§]mcule.com Ltd., Vendel utca 15−17. B/2/6, H-1096 Budapest, Hungary

[∥]NanGenex Inc., Záhony u. 7. H-1031 Budapest, Hungary


## ■ ACKNOWLEDGMENTS

We thank to Peter Oledzki for his useful comments during the evaluation of FTrees, Zoltán Béni for NMR measurements, and Márton Vass for his assistance in the preparation of the manuscript.

## ■ ABBREVIATIONS:

H4, histamine H4 receptor; SERT, serotonin transporter; EF, enrichment factor; HTS, high-throughput screening

## ■ REFERENCES


(1) Evers, A.; Hessler, G.; Matter, H.; Klabunde, T. Virtual screening of biogenic amine-binding G-protein coupled receptors: Comparative evaluation of protein- and ligand-based virtual screening protocols. *J. Med. Chem.* **2005**, *48*, 5448−5465.

(2) Wu, J. S.; Peng, Y. H.; Wu, J. M.; Hsieh, C. J.; Wu, S. H.; Coumar, M. S.; Song, J. S.; Lee, J. C.; Tsai, C. H.; Chen, C. T.; Liu, Y. W.; Chao, Y. S.; Wu, S. Y. Discovery of non-glycoside sodium-dependent glucose co-transporter 2 (SGLT2) inhibitors by ligand-based virtual screening. *J. Med. Chem.* **2010**, *53*, 8770−8774.

(3) Onnis, V.; Kinsella, G. K.; Carta, G.; Jagoe, W. N.; Price, T.; Williams, D. C.; Fayne, D.; Lloyd, D. G. Virtual screening for the identification of novel nonsteroidal glucocorticoid modulators. *J. Med. Chem.* **2010**, *53*, 3065−3074.

(4) Chiang, Y. K.; Kuo, C. C.; Wu, Y. S.; Chen, C. T.; Coumar, M. S.; Wu, J. S.; Hsieh, H. P.; Chang, C. Y.; Jseng, H. Y.; Wu, M. H.; Leou, J. S.; Song, J. S.; Chang, J. Y.; Lyu, P. C.; Chao, Y. S.; Wu, S. Y. Generation of ligand-based pharmacophore model and virtual screening for identification of novel tubulin inhibitors with potent anticancer activity. *J. Med. Chem.* **2009**, *52*, 4221−4233.

(5) Ripphausen, P.; Nisius, B.; Peltason, L.; Bajorath, J. Quo vadis, virtual screening? A comprehensive survey of prospective applications. *J. Med. Chem.* **2010**, *53*, 8461−8467.

(6) Kiss, R.; Kiss, B.; Könczöl, A.; Szalai, F.; Jelinek, I.; László, V.; Noszál, B.; Falus, A.; Keserű, G. M. Discovery of novel human histamine H4 receptor ligands by large-scale structure-based virtual screening. *J. Med. Chem.* **2008**, *51*, 3145−3153.

(7) Kiss, R.; Polgár, T.; Kirabo, A.; Sayyah, J.; Figueroa, N. C.; List, A. F.; Sokol, L.; Zuckerman, K. S.; Gali, M.; Bisht, K. S.; Sayeski, P. P.; Keserű, G. M. Identification of a novel inhibitor of JAK2 tyrosine kinase by structure-based virtual screening. *Bioorg. Med. Chem. Lett.* **2009**, *19*, 3598−3601.

(8) Kovac, A.; Konc, J.; Vehar, B.; Bostock, J. M.; Chopra, I.; Janezic, D.; Gobec, S. Discovery of new inhibitors of D-alanine: D-alanine ligase by structure-based virtual screening. *J. Med. Chem.* **2008**, *51*, 7442−7448.

(9) Geldenhuys, W. J.; Darvesh, A. S.; Funk, M. O.; Van der Schyf, C. J.; Carroll, R. T. Identification of novel monoamine oxidase B inhibitors by structure-based virtual screening. *Bioorg. Med. Chem. Lett.* **2010**, *20*, 5295−5298.

(10) Ruda, G. F.; Campbell, G.; Alibu, V. P.; Barrett, M. P.; Brenk, R.; Gilbert, I. H. Virtual fragment screening for novel inhibitors of 6-phosphogluconate dehydrogenase. *Bioorg. Med. Chem.* **2010**, *18*, 5056−5062.

(11) Schneider, G.; Neidhart, W.; Giller, T.; Schmid, G. "Scaffold-Hopping" by topological pharmacophore search: A contribution to virtual screening. *Angew. Chem., Int. Ed. Engl.* **1999**, *38*, 2894−2896.

(12) Rarey, M.; Dixon, J. S. Feature Trees: A new molecular similarity measure based on tree matching. *J. Comput. Aided Mol. Des.* **1998**, *12*, 471−490.

(13) Briem, H.; Lessel, U. F. In vitro and in silico affinity fingerprints: Finding similarities beyond structural classes. *Perspect. Drug Discov.* **2000**, *20*, 231−244.

(14) Cheng, Y. C.; Prusoff, W. H. Relationship between the inhibition constant ($K_i$) and the concentration of inhibitor which causes 50% inhibition ($IC_{50}$) of an enzymatic reaction. *Biochem. Pharmacol.* **1973**, *22*, 3099−3108.

(15) D'Amato, R. J.; Largent, B. L.; Snowman, A. M.; Snyder, S. H. Selective labeling of serotonin uptake sites in rat brain by [$^3$H]citalopram contrasted to labeling of multiple sites by [$^3$H]imipramine. *J. Pharmacol. Exp. Ther.* **1987**, *242*, 364−371.

(16) Owens, M. J.; Morgan, W. N.; Plott, S. J.; Nemeroff, C. B. Neurotransmitter receptor and transporter binding profile of antidepressants and their metabolites. *J. Pharmacol. Exp. Ther.* **1997**, *283*, 1305−1322.

(17) Wild, D. J.; Blankley, C. J. Comparison of 2D fingerprint types and hierarchy level selection methods for structural grouping using Ward's clustering. *J. Chem. Inf. Comput. Sci.* **2000**, *40*, 155−162.

(18) Bender, A.; Mussa, H. Y.; Glen, R. C.; Reiling, S. Similarity searching of chemical databases using atom environment descriptors (MOLPRINT 2D): Evaluation of performance. *J. Chem. Inf. Comput. Sci.* **2004**, *44*, 1708−1718.

(19) Baringhaus, K. H.; Hessler, G. Fast similarity searching and screening hit analysis. *Drug Discovery Today* **2004**, *1*, 197−202.

(20) Smits, R. A.; Lim, H. D.; Hanzer, A.; Zuiderveld, O. P.; Guaita, E.; Adami, M.; Coruzzi, G.; Leurs, R.; de Esch, I. J. Fragment based design of new H4 receptor-ligands with anti-inflammatory properties in vivo. *J. Med. Chem.* **2008**, *51*, 2457−2467.

(21) Smits, R. A.; de Esch, I. J. P.; Zuiderveld, O. P.; Broeker, J.; Sansuk, K.; Guaita, E.; Coruzzi, G.; Adami, M.; Haaksma, E.; Leurs, R. Discovery of quinazolines as histamine H4 receptor inverse agonists using a scaffold hopping approach. *J. Med. Chem.* **2008**, *51*, 7855−7865.

(22) Sander, K.; Kottke, T.; Tanrikulu, Y.; Proschak, E.; Weizel, L.; Schneider, E. H.; Seifert, R.; Schneider, G.; Stark, H. 2,4-Diaminopyrimidines as histamine H4 receptor ligand: Scaffold optimization and pharmacological characterization. *Bioorg. Med. Chem.* **2009**, *17*, 7186−7196.

(23) Cramp, S.; Dyke, H. J.; Higgs, C.; Clark, D. E.; Gill, M.; Savy, P.; Jennings, N.; Price, S.; Lockey, P. M.; Norman, D.; Porres, S.; Wilson, F.; Jones, A.; Ramsden, N.; Mangano, R.; Leggate, D.; Andersson, M.; Hale, R. Identification and hit-to-lead exploration of a novel series of

histamine H4 receptor inverse agonists. *Bioorg. Med. Chem. Lett.* **2010**, *20*, 2516−2519.
(24) Jablonowski, J. A.; Grice, C. A.; Chai, W.; Dvorak, C. A.; Venable, J. D.; Kwok, A. K.; Ly, K. S.; Wei, J.; Baker, S. M.; Desai, P. J.; Jiang, W.; Wilson, S. J.; Thurmond, R. L.; Karlsson, L.; Edwards, J. P.; Lovenberg, T. W.; Carruthers, N. I. The first potent and selective non-imidazole human histamine H4 receptor antagonists. *J. Med. Chem.* **2003**, *46*, 3957−3960.
(25) Sato, H.; Tanaka, K.; Shimazaki, M.; Urbahns, K.; Sakai, K.; Gantner, F.; Bacon, K. 2-Aminopyrimidine Derivatives. Bayer Healthcare AG., WO2005054239, 2005.
(26) Sato, H.; Fukushima, K.; Shimazaki, M.; Urbahns, K.; Sakai, K.; Gantner, F.; Bacon, K. 2-Aminopyrimidine Derivatives. Bayer Healthcare AG., WO2005014556, 2005.
(27) Ballesteros, J. A.; Weinstein, H. Integrated methods for the construction of three-dimensional models and computational probing of structure-function relations in G protein-coupled receptors. *Methods Neurosci.* **1995**, *25*, 366−428.
(28) Kiss, R.; Noszál, B.; Rácz, A.; Falus, A.; Erős, D.; Keserű, G. M. Binding mode analysis and enrichment studies on homology models of the human histamine H4 receptor. *Eur. J. Med. Chem.* **2008**, *43*, 1059−1070.
(29) Jongejan, A.; Lim, H. D.; Smits, R. A.; de Esch, I. J.; Haaksma, E.; Leurs, R. Delineation of agonist binding to the human histamine H4 receptor using mutational analysis, homology modeling, and ab initio calculations. *J. Chem. Inf. Model.* **2008**, *48*, 1455−1463.
(30) Pae, A. N.; Cho, Y. S.; Choo, H.; Kim, H.; Koh, H. Y.; Park, W.; Kong, J. Y.; Chae, M. Y.; Cho, I.; Hwang, B. W.; Lee, D. H. Use of N-benzyl-N-(2-dimethylamino-ethyl)benzenesulfonamide Derivatives for Treating Central Nervous System Disorders. *Dongbu Hitek Co., Ltd.* WO2008093919A1, 2008.
(31) Manepalli, S.; Geffert, L. M.; Surratt, C. K.; Madura, J. D. Discovery of novel selective serotonin reuptake inhibitors through development of a protein-based pharmacophore. *J. Chem. Inf. Model.* **2011**, *51*, 2417−2426.
(32) Gundertofte, K.; Bogeso, K. P.; Liljefors, T. A stereoselective pharmacophoric model of the serotonin reuptake site. In *Computer-Assisted Lead Finding and Optimization*; van de Waterbeemd, H., Testa, B., Folkers, G., Eds.; Verlag Helvetica Chimica Acta (VHCA): Basel, 1997; pp 443−459.
(33) Rupp, A.; Kovar, K. A.; Beuerle, G.; Ruf, C.; Folkers, G. A new pharmophoric model for 5-HT reuptake-inhibitors: Differentiation of amphetamine analogues. *Pharm. Acta Helv.* **1994**, *68*, 235−244.
(34) Lindberg, U. H.; Thorberg, S. O.; Bengtsson, S.; Renyi, A. L.; Ross, S. B.; Ogren, S. O. Inhibitors of neuronal monoamine uptake. 2. Selective inhibition of 5-hydroxytryptamine uptake by alpha-amino acid esters of phenethyl alcohols. *J. Med. Chem.* **1978**, *21*, 448−456.
(35) Chang, A. S.; Chang, S. M.; Starnes, D. M. Structure-activity relationships of serotonin transport: Relevance to nontricyclic antidepressant interactions. *Eur. J. Pharmacol.* **1993**, *247*, 239−248.